Engineering Structures 183 (2019) 523–532

Contents lists available at ScienceDirect

Engineering Structures

journal homepage: www.elsevier.com/locate/engstruct

Axial capacity of steel tube-reinforced concrete stub columns

Huan-Peng Hong[a], Huang Yuan[a,*], Lu Deng[a], Yu Bai[b]

[a] Key Laboratory for Damage Diagnosis of Engineering Structures of Hunan Province, College of Civil Engineering, Hunan University, Changsha 410082, People's Republic of China

[b] Department of Civil Engineering, Monash University, Clayton, VIC 3800, Australia

ARTICLE INFO

Keywords:
Steel tube-reinforced concrete columns
Axial capacity
Stress and strain analysis
Lateral confinement

ABSTRACT

The steel tube-reinforced concrete (ST-RC) column is an innovative composite structure that has been increasingly applied in high-rise buildings and bridge piers in China. This study aims to investigate the axial capacity of the ST-RC stub column by means of a modified superposition method. Primarily, the sectional confining force equilibrium was elaborated to explain the confinement mechanism of the ST-RC column under concentric compression, which involves the confining stress induced from the inner steel tube and secondary confining stress induced from the peripheral steel hoops. Thereafter, a modified method for predicting the axial capacity of the ST-RC column, considering the secondary confinement, was developed according to a stress and strain analysis. Thirdly, 41 published specimens were collected to verify the accuracy of the proposed method. It was demonstrated that the current method fitted strongly with the tests results and exhibited satisfactory adaptability. Finally, four other methods according to ACI 318, AIJ, EC 4, and CECS 188-2005 were verified in the same scenario. It was found that the current method exhibited superior correlation with the experimental results compared with conventional approaches. It will be favorable to obtain the viable axial capacity of the ST-RC column by using the presented solution.

1. Introduction

A steel tube-reinforced concrete (ST-RC) column refers to a composite column in which a concrete-filled steel tube (CFST) is embedded in the reinforced concrete (RC). Fig. 1 illustrates the typical cross-section and internal structure of an ST-RC column in an actual project. The ST-RC column effectively combines the respective advantages of CFST and RC columns. Owing to its superior structural performance, the ST-RC column has gained popularity in high-rise buildings and bridge piers in earthquake-prone regions of China [1–4]. Nevertheless, as an innovative type of composite structure, there remains a lack of information regarding the confinement mechanism of the ST-RC column under axial compression; discrepancies also exist in its axial capacity prediction provided in different leading design methods. These all highlight the need for the development of an accurate and well-defined method for predicting the axial capacity of ST-RC columns.

Previous tests and studies have shown that the strength and ductility of concrete columns are highly dependent on the lateral confinement level [5–8]. When transverse confinement is provided effectively, the axial capacity and compressive performance of the concrete can be improved considerably. In general, the confinement provided by hoops, crossties or steel tubes is considered as passive; that is, lateral confinement reacts to the lateral concrete dilation under an axial load. By comparing the responses under both active and passive confinement, it was confirmed by Richart et al. [9] that these two types of behaviors are similar. Mander et al. [10] suggested that the relation between the axial strength and confining stress can be described as:

$$\sigma_{cr} = f_0 + k_1\sigma_r \tag{1}$$

where σ_{cr} denotes the strength of the confined concrete; f_0 denotes the concrete strength without considering the confinement effect; σ_r denotes the confining stress; and the coefficient k_1 denotes the increment in the concrete strength owing to lateral confinement. Different researchers have suggested different values for k_1. Richart et al. [9] investigated the relationship between k_1 and σ_r by means of experiments, and Fig. 2 presents the tests results. It can be concluded that the coefficient k_1 is approximately equal to 4.1 when the lateral confinement is larger than 20 MPa. For a small value of lateral pressure in a confined concrete column, k_1 is larger than the commonly adopted value of 4.1. By means of regression analysis of the test data, Eq. (2) obtained by Razvi et al. [11] revealed the variation in k_1 with the lateral confining stress σ_r, which exhibited strong adaptability, as depicted in Fig. 2.

$$k_1 = 6.7(\sigma_r)^{-0.17} \tag{2}$$

* Corresponding author.
E-mail address: huangy@hnu.edu.cn (H. Yuan).

https://doi.org/10.1016/j.engstruct.2019.01.044
Received 27 August 2018; Received in revised form 18 December 2018; Accepted 9 January 2019

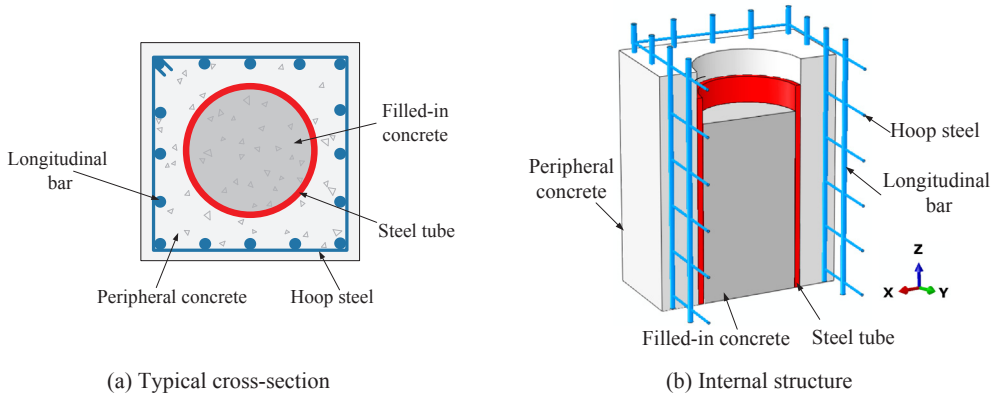

Fig. 1. Typical structure of ST-RC column.

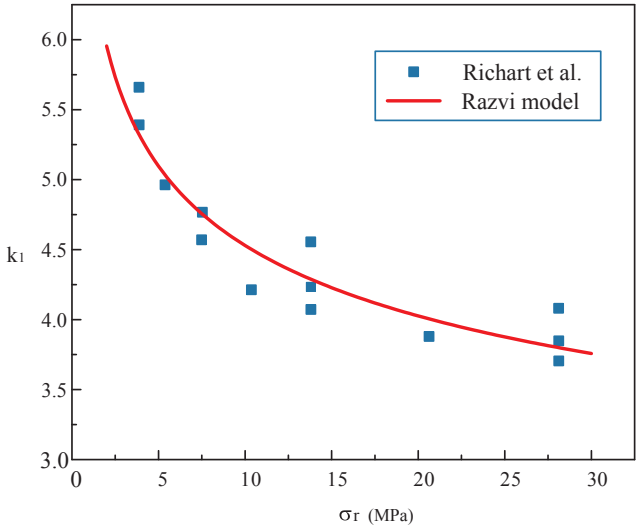

Fig. 2. Variations in coefficient k_1 with confining stress.

To improve the brittle performance of the concrete column and take advantage of the lateral confinement, various types of lateral confinement configurations have been applied [12–17], such as circular hoops, rectangular hoops with crossties, steel tubes, and fiber-reinforced polymer (FRP) strips. Among these, the CFST column is a highly effective composite structure that employs the respective advantages of both the steel tube and filled-in concrete. With the strong lateral confining pressure provided by the steel tube, the filled-in concrete exists under the triaxial stress state and behaves with higher strength. Studies have been conducted to learn the behavior of CFST columns over the past decades [18,19]. Nevertheless, the conventional CFST system exhibits certain disadvantages in practice, such as complicated beam-to-column connections, poor resistance against fire or corrosion, as well as the easy occurrence of outward local buckling [20–22], which have limited its application popularity to a certain extent.

Under this circumstance, a new composite system, namely the ST-RC column, was proposed and has been widely used in actual projects in China. On the one hand, compared with the conventional CFST column, the ST-RC column offers the following advantages: easier beam-to-column connections, superior lateral stiffness and ductility, higher fire resistance, and improved corrosion protection, effectively prohibiting outward buckling owing to the confinement of the peripheral RC encasement. On the other hand, the ST-RC column is also superior to the conventional RC column. With the presence of the inner CFST, the ST-RC column offers higher lateral stiffness and axial strength than the conventional RC column.

Considerable efforts have been devoted to the investigation of ST-RC columns. Thus far, studies including both experimental testing and numerical simulation have been conducted. Ji et al. [1] examined the seismic behavior of ST-RC columns, and developed formulae for the capacity of ST-RC columns under seismic loads based on the superposition method. Nie et al. [2] proposed a new connection system for the ST-RC column and RC beams. Axial compression experiments and reversed cyclic loading tests were conducted. The corresponding load-deflection performance, typical failure modes, stress and strain distributions, and energy dissipation capacity of the proposed beam-column system were obtained. Ji et al. [3] investigated the effects of the cumulative seismic damage of ST-RC columns; recommendations were made for the amount of transverse reinforcement required in the seismic design of ST-RC columns to ensure adequate deformation capacity. Han et al. [23] studied the tensile behavior of the ST-RC column by experimental investigation and full-range finite element analysis. The authors investigated the bond strength between the steel tubes and proposed a simplified model for predicting the tensile strength of ST-RC columns. Han and An [24] studied the behavior of ST-RC columns under axial compression by means of finite element analysis. The interactions between the outer concrete and steel tube of the CFST, as well as the core concrete and steel tube of the CFST, were investigated. By analyzing different design codes, a superior method was suggested for predicting the ultimate strength of the composite stub columns. Huang et al. [25] investigated the nonlinear behavior of a staged construction ST-RC column using finite element analysis, and a verified formula was developed for calculating the displacement ductility of staged construction ST-RC. The demand for displacement ductility under different seismic grades was also presented. In view of the previous studies, most theories for predicting the bearing capacity of the ST-RC column were based on adding the capacity of the outer RC and inner CFST separately, without considering the interaction between these two components [24,26].

A number of studies were conducted to investigate the effects of secondary confinement on composite columns. The first formulation taking account of secondary confinement was proposed by Karabinis and Rousakis [27], who suggested evaluating the ultimate strength of confined concrete by means of superimposing twofold lateral confinement: the first accounts for the effect of the steel hoops, while the second accounts for the effect of the FRP strips. Since then, the double confinement effects of different structural elements, including the steel tube and steel hoops, steel angle and battens, steel hoops and FRP strips, and steel hoops and steel section, have been extensively studied and confirmed [28–32]. Montuori and Piluso [28] studied the behavior of RC columns confined by means of steel angles and battens, where the effect of the steel angle and secondary effect of the battens were accounted for. In the prediction of the bearing capacity of reinforced concrete sections strengthened by FRP wrapping, the effect of the original steel hoops and secondary effect of the FRP fiber were considered

[29,30]. He et al. [31] studied the behavior of steel-jacket retrofitted RC columns by means of experiments and fiber element analysis, in which the effects of both the steel jacket and original steel hoops were considered. In the study of steel-reinforced concrete (SRC) columns, according to Chen and Wu [32], the concrete in an SRC cross-section can be divided into three parts, according to the confinement effectiveness, effect of the core steel section with flanges, and secondary effect of the outer steel hoops, which were incorporated into the analytical model. However, existing studies have not thoroughly investigated the confining mechanism of ST-RC columns. As the level of lateral confinement considerably affects the concrete strength, utilizing the existing theories without considering the interaction between the CFST and RC components may lead to inaccurate ST-RC column predictions. This necessitates further research on the confinement mechanism and axial capacity of ST-RC columns under axial compression.

Therefore, this study considers the secondary confinement and proposes a modified superposition method for predicting the axial capacity of the ST-RC column. The key objectives of this research were fourfold: firstly, the sectional confining pressure equilibrium was developed to explain the confinement mechanism of the ST-RC column under concentric compression; secondly, a modified method for predicting the axial capacity of ST-RC columns was obtained through stress and strain analyses, based on the sectional confining pressure equilibrium; thirdly, a large number of published experimental specimens were used to verify the adaptability of the proposed method, and the comparison between experimental and predicted results demonstrated strong agreement, pointing out the accuracy of the proposed method; finally, four other methods according to ACI 318-14, AIJ, Eurocode 4-2004, and CECS 188-2005 were verified using the same scenario.

2. Confining stresses in ST-RC column

2.1. Equilibrium condition of ST-RC column

The validity of numerical techniques for confined concrete relies on the utilization of an accurate lateral confining pressure model. The lateral confining pressure depends on both the material properties and geometries of the column. Compared with conventional RC and CFST columns, the ST-RC column contains both an inner CFST core and an outer RC encasement, and the filled-in concrete is in the triaxial compressive stress state when the column is subjected to compressive loading. A schematic view of the confining stress system of an axially loaded ST-RC column in the equilibrium condition is illustrated in Fig. 3. It can be observed that the core CFST is constricted by the confining pressure provided by the peripheral stirrups. The confinement effects on the core concrete can be divided into two parts: the confinement of the steel tube and effective confinement of the outer steel hoops, as illustrated in Fig. 4, where σ_l and σ_θ denote the tensile stresses of the peripheral stirrups and core steel tube, respectively. Thus, the effective confining pressure f_e on the filled-in concrete can be expressed by:

$$f_e = f_r + f_{le} \tag{3}$$

where f_r represents the confining stress of the steel tube, and f_{le} represents the effective confining stress of the peripheral steel hoops. In this study, it was assumed that all materials of the ST-RC column were isotropic, and the axial strains of the steel and concrete were considered to be identical under concentric compression, according to the plane section assumption.

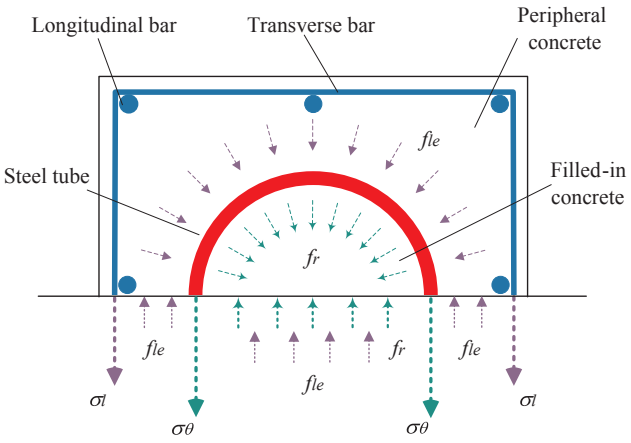

Fig. 4. Equilibrium relationship of ST-RC column.

2.2. Determination of f_r

A schematic view of the core CFST component is presented in Fig. 5. Based on the sectional force equilibrium condition, the lateral confining

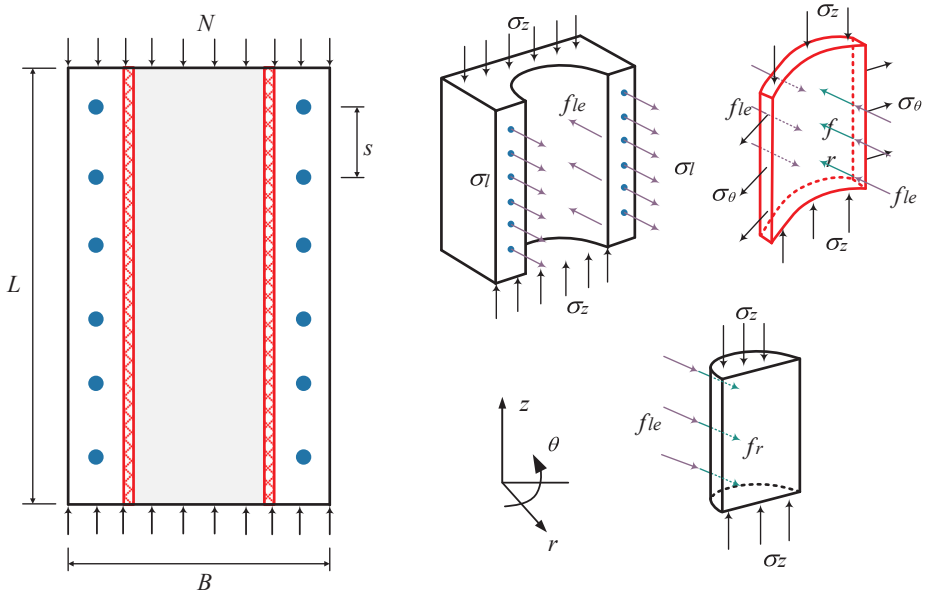

Fig. 3. Confining stress system of ST-RC column.

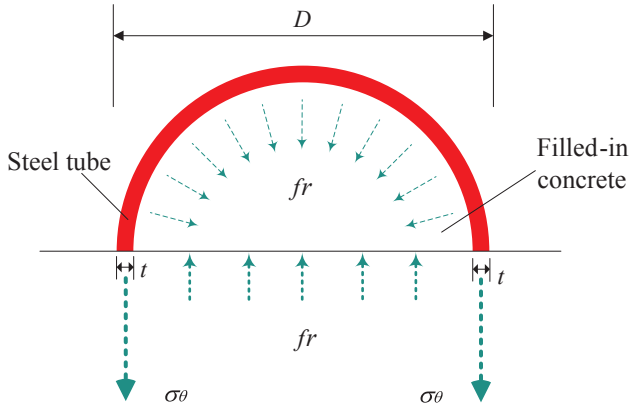

Fig. 5. Equilibrium relationship of CFST column.

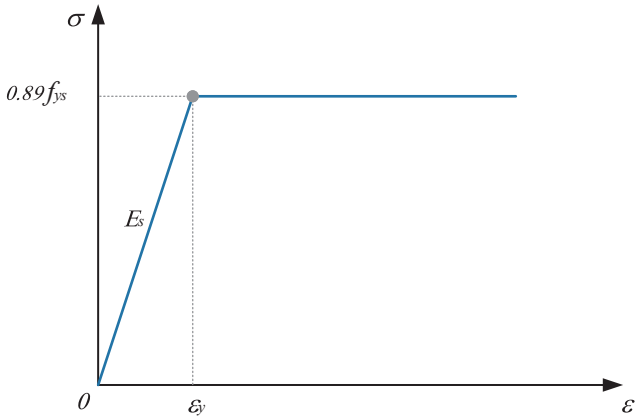

Fig. 6. Uniaxial stress–strain relationship of steel tube.

stress f_r provided by the steel tube can be obtained by:

$$f_r(D - 2t) = 2\sigma_\theta t \tag{4}$$

which can be rewritten as:

$$f_r = \frac{2\sigma_\theta t}{(D - 2t)} \tag{5}$$

where t and D denote the thickness and diameter of the steel tube, respectively; and σ_θ denotes the hoop stress of the steel tube.

The steel tube in the CFST column is biaxially stressed owing to the confinement effect. The presence of the hoop tension will reduce its yield stress along the longitudinal direction [33]. For the sake of simplicity, the hoop stress σ_θ and longitudinal stress σ_z of the steel tube in the yield condition are generally assumed to be:

$$\sigma_\theta = \alpha_u \sigma_{ys} \text{ and } \sigma_z = \beta_u \sigma_{ys} \tag{6}$$

where α_u and β_u represent the reduction coefficients, and σ_{ys} denotes the yield strength of the steel tube.

When the steel tube is subjected to multiple stresses, a von Mises yield criterion can be employed to define the limit state, expressed as:

$$\sigma_\theta^2 - \sigma_\theta \sigma_z + \sigma_z^2 = \sigma_{ys}^2 \tag{7}$$

which can be rewritten as:

$$\alpha_u^2 - \alpha_u \beta_u + \beta_u^2 = 1 \tag{8}$$

Different researchers have recommended different values for the reduction coefficients α_u and β_u [34,35]. According to Sakino et al. [34], the relation between the reduction coefficients α_u and β_u can be described by:

$$\gamma = \beta_u - 1 - \frac{D - 2t}{2(D - 2t)} 4.1\alpha_u \tag{9}$$

where γ denotes the augmentation factor and the value of $\gamma = 0.27$ was recommended. Assuming $D/t = 50$ as a representative value to avoid the dependency of α_u and β_u on the D/t ratio, the values of α_u and β_u can be determined by solving Eqs. (8) and (9) simultaneously. From a theoretical perspective, the values $\alpha_u = -0.19$ and $\beta_u = 0.89$ were adopted, and further details can be found in [34]. The uniaxial stress–strain relationship of the steel tube is assumed to be elastic-perfectly plastic, as illustrated in Fig. 6.

2.3. Determination of f_{le}

For the concrete column confined with square hoops, previous investigators have pointed out that the confining stress distribution on the cross-section and along the axial direction are complicated, because the lateral dilation of the confined concrete is localized [8,10]. When the confined concrete expands laterally under axial compression, the restraining force near the corners and longitudinal bars is higher than that between the corners and longitudinal bars, as the area near the corner and supported longitudinal bars can provide stronger support to the hoop steel. A schematic view of the confining pressure distribution in the RC column is illustrated in Fig. 7.

Numerous approaches have been proposed to determine the confinement effect of stirrups [7,8,10,11]. Mander et al. [10] pointed out that the axial variation in the confining pressure is assumed to occur in the form of a second-degree parabola with an initial tangent slope of 45°, which is accurate yet rather complicated in application. According to Saatcioglu et al. [8], the confining pressure near the hoop steel nodes, where the longitudinal bar is supported by stirrups, is distributed fairly uniformly along the length of the longitudinal bar. The reason is that the longitudinal bar is restricted by the hoop steel at the nodal point and will maintain the restraining action until outward bulking occurs. When the reinforcement is closely spaced, the unrestricted

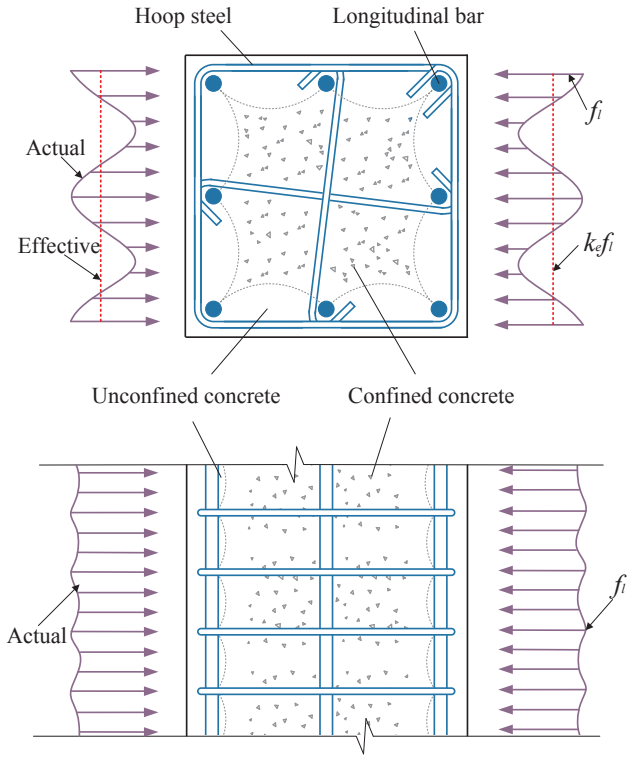

Fig. 7. Confining stress distribution of RC column.

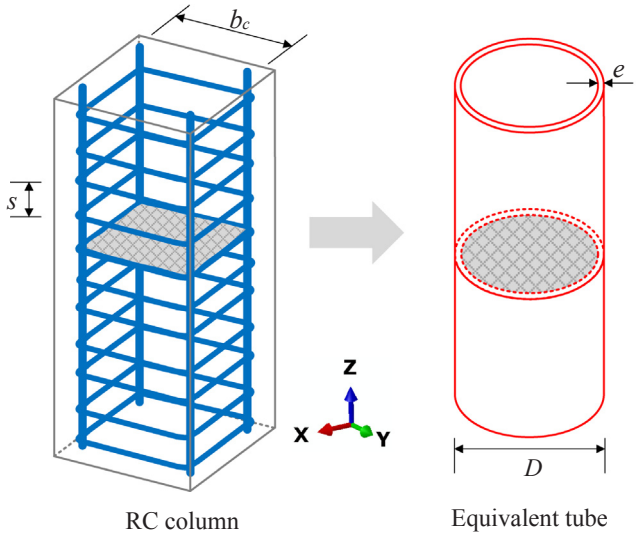

Fig. 8. Equivalent tube concept.

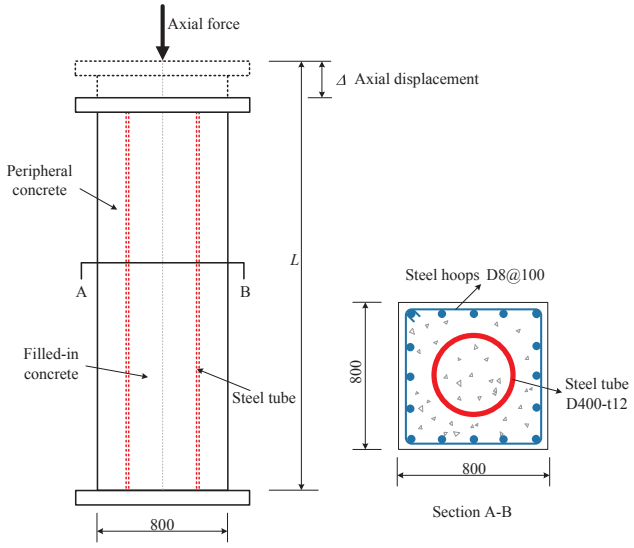

Fig. 9. Details of typical ST-RC specimen and loading program.

length of the longitudinal bar is short between the ties; thus, the pressure distribution along the length is close to uniform.

To provide an improved representation of the confining stress distribution of RC, the concept of the "equivalent circular tube", proposed by Legeron et al. [7], was adopted. The diameter of the equivalent circular column D was equal to the size of the concrete core of the rectangular column measured center-to-center of the outer tie in the studied direction. Fig. 8 presents a schematic view of the equivalent tube concept. For the circular column with a diameter D, the thickness of the equivalent circular tube e is:

$$e = k_e \frac{nA_{yv}}{2s} \tag{10}$$

where k_e denotes the confinement effectiveness coefficient; A_{yv} denotes the cross-sectional area of hoops; n denotes the number of legs in the calculated direction; and s denotes the tie spacing.

The confinement effectiveness coefficient proposed by Saatcioglu et al. [8] was adopted.

$$k_e = 0.26\sqrt{\left(\frac{b_c}{s}\right)\left(\frac{b_c}{s_l}\right)\left(\frac{1}{f_l}\right)} \tag{11}$$

where b_c denotes the core dimension measured center-to-center of the perimeter hoop; s_l denotes the spacing of the longitudinal reinforcement; s denotes the spacing of the transverse hoops; f_{yv} denotes the yield strength of the stirrups; and f_l denotes the average confinement pressure, expressed as:

$$f_l = \frac{nA_{yv}f_{yv}}{sb_c} \tag{12}$$

Thus, according to the force equilibrium and strain compatibility on the cross-section illustrated in Fig. 5, the effective confining stress f_{le} provided by the reinforcement hoops can be calculated as:

$$f_{le} = \frac{2ef_{yv}}{D - 2e} \tag{13}$$

3. Axial capacity of ST-RC stub columns

In practical application, reliable design of the ST-RC column necessitates an accurate yet well-defined method to predict its axial capacity. In past decades, the superposition method has been used extensively to predict the axial capacity of SRC columns in Japan and China [36,37], demonstrating satisfactory accuracy and simplicity. In the conventional superposition method, the axial capacities of the outpacked concrete and steel section were added separately, without considering the interaction between interfaces. Based on the concept of the conventional superposition method for the SRC column, a modified method taking into account the secondary confinement was developed for predicting the axial capacity of the ST-RC columns in the current study.

To investigate the mechanism of the ST-RC column further, a typical ST-RC stub column in a real high-rise building was designed, which was obtained from a 26-story frame-shear wall structure. The parameters of the typical column are as follows: cross-section length $B = 800$ mm; for the inner CFST component, outer diameter of steel tube $D = 400$ mm, thickness $t = 12$ mm, yield strength of steel tube $f_{ys} = 345$ MPa, compressive strength of filled-in concrete $f_{01} = 70$ MPa; for the outer RC component, compressive strength of outer concrete $f_{02} = 50$ MPa, yield strength of longitudinal bar $f_{yl} = 400$ MPa, $s_l = 184$ mm, $n = 5$, the stirrup diameter of was 12 mm, space $s = 100$ mm, and yield strength of stirrups $f_{yv} = 345$ MPa. The axial strain of the inner CFST and outer RC components were equal to $\varepsilon = \Delta/L$, in which L denotes the length of the ST-RC column and Δ denotes the axial compressive displacement. Fig. 9 presents a schematic view of the cross-section configuration and loading program of the typical ST-RC column.

The typical axial force versus axial strain relationships of the ST-RC components, including the peripheral RC and core CFST, are illustrated in Fig. 10. Three characteristic points are marked on the curve, namely point A, where the steel tube transformed into the elastic-plastic stage, point B, where the outer RC component reached its peak strain; and point C, where the inner CFST component reached its peak strain. Therefore, the typical axial force–strain curve of the ST-RC column can be divided into three stages.

- Stage 1 (OA): The ST-RC column and its components exhibited elastic behavior in this stage. The stress of the outer RC was approximately 70% of its peak strength, and the stress of the core filled-in concrete was approximately 65% of its peak strength. The steel tube entered the elastic-plastic stage after point A.
- Stage 2 (AB): During this stage, the overall trend of the ST-RC column was upward. The steel tube entered the plastic stage and leveled off, but the forces of the outer RC and inner CFST continued to ascend with the increment in the axial strain.
- Stage 3 (BC): The outer RC reached its ultimate strength at point B and the ST-RC also attained its peak strength. Thereafter, the capacity of the ST-RC began to decline along with the descending of

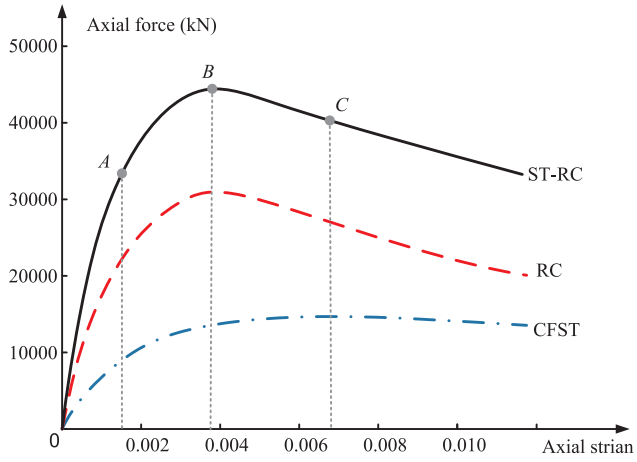

Fig. 10. Axial force-strain relationships of ST-RC components.

the RC component, despite the small increment in the core CFST. The ultimate limit state of the ST-RC is defined as the peak strain of the outer RC, denoted by point B in Fig. 10.

In the ST-RC column, the peak strain of the core CFST component is generally higher than the peak strain of the outer RC component, because the lateral confinement provided by the steel tube is more effective than that provided by separate stirrups [38,39]. Thus, the axial force-strain curve of the core CFST continued to ascend after the outer RC reached its peak strain (point B) under axial compression. Nevertheless, as the peripheral RC generally accounts for a greater cross-sectional area than the core CFST, and the increment of the core CFST from points B to C is relatively small, the decrease in the outer RC cannot be offset. As a result, the overall trend of the ST-RC column force-strain curve will decline with the decrease in the outer RC after reaching the RC peak strain. Therefore, point B can be determined as the ultimate limit state of the ST-RC column.

Therefore, a modified superposition method was developed for predicting the axial capacity of the ST-RC column. The current method was conducted by superimposing the respective bearing capacities of the core CFST and outer RC at the ultimate limit state, while the secondary confinement of the filled-in concrete was considered. Prior to implementing the method, two additional assumptions were adopted, as follows:

- Under axial compression, the axial strain distribution is uniform in the cross-section, according to the flat section assumption, which has been confirmed by Kang et al. [40].
- Only the case of the stub column (with a ratio of specimen height to sectional length of no more than 3) was considered in the current study.

The definition of the ultimate limit state of the ST-RC relies on the utilization of accurate constitutive models for both the CFST and RC components. To predict the axial capacity of the ST-RC column accurately, with a large number of calculations and substantial verification, the widely accepted constitutive model for concrete confined by transverse reinforcement, proposed by Razvi et al. [11], and the constitutive model for the CFST column, proposed by Sakino et al. [34], were adopted in this study.

3.1. Outer RC

The peak strain of the hoop-confined RC ε_1 is expressed as [11]:

$$\varepsilon_1 = \varepsilon_{01}(1 + 5k_2K_1) \tag{14}$$

and the strength enhancement coefficient K_1 is given by:

$$K_1 = \frac{k_1 f_{le}}{f_{01}} \tag{15}$$

where ε_{01} and f_{01} are the peak strain and compressive strength of the outer concrete encasement without considering the confinement effect, respectively, expressed as:

$$\varepsilon_{01} = 0.0028 - 0.0008k_2 \tag{16}$$

$$k_2 = \frac{40}{f_{01}} \tag{17}$$

where k_2 is the coefficient reflecting the effects of the increased concrete strength.

Following Eq. (1), the peak stress of the outer RC f_1 can be determined as:

$$f_1 = f_{01} + k_1 f_{le} \tag{18}$$

Thus, the bearing capacity of the outer RC is obtained by:

$$N_{RC} = f_1 A_{RC} + f_{yl} A_{yl} \tag{19}$$

where A_{RC} and A_{yl} are the sectional areas of the outer RC encasement and longitudinal bars, and f_{yl} denotes the yield strength of the longitudinal bars.

3.2. Core CFST

The stress of the core filled-in concrete f_{c2} corresponding to the ultimate limit state of the ST-RC column can be obtained from the following formulae [34]:

$$f_{c2} = f_2 \left[\frac{VX + (W-1)X^2}{1 + (V-2)X + WX^2} \right] \tag{20}$$

where

$$X = \frac{\varepsilon_2}{\varepsilon_{02}} \tag{21}$$

$$f_2 = f_{02} K_2 \tag{22}$$

$$K_2 = 1 + 4.1\frac{f_e}{f_{02}} \tag{23}$$

$$W = 1.50 - 0.0171 f_{02} + 2.39 f_e^{0.5} \tag{24}$$

$$V = \frac{E_c \varepsilon_{02}}{f_{02}} \tag{25}$$

$$E_c = (6.9 + 3.32 f_{02}^{0.5}) * 10^{-3} \tag{26}$$

The effective confining pressure f_e of the filled-in concrete can be found in Eq. (3). The peak strain of the CFST, ε_2, is expressed as [34]:

$$\text{when } K_2 < 1.5, \quad \varepsilon_2 = \varepsilon_{02}[1 + 4.7(K_2 - 1)] \tag{27}$$

$$\text{when } K_2 < 1.5, \quad \varepsilon_2 = \varepsilon_{02}[3.4 + 20(K_2 - 1)] \tag{28}$$

$$\text{in which} \quad \varepsilon_{02} = 0.00094(f_{02})^{0.25} \tag{29}$$

where f_{02} denotes the compressive strength of the filled-in plain concrete.

Thus, the bearing capacity of the core CFST is obtained by:

$$N_{CFST} = f_{c2} A_{core} + 0.89 f_{ys} A_{ys} \tag{30}$$

where A_{core} and A_{ys} are the sectional areas of the filled-in concrete and steel tube, respectively; the uniaxial stress–strain relationship of the steel tube is assumed to be elastic-perfectly plastic, and the maximum stress of the steel tube is 0.89 f_{ys}, as depicted in Fig. 6.

3.3. ST-RC column

Therefore, the axial capacity of the ST-RC column can be determined by performing the following steps.

- (1) Determine the peak strain (ε_1) and peak stress (f_1) of the peripheral RC by Eqs. (14) and (18), respectively.
- (2) Obtain the stress of the CFST (f_{c2}), corresponding to the strain (ε_1), by Eq. (20).
- (3) Calculate the respective strengths of the RC and CFST components by means of Eqs. (19) and (30). Thus, the axial capacity of the ST-RC column can be determined as:

$$N' = N_{RC} + N_{CFST} \tag{31}$$

4. Verification of proposed method

To validate the proposed numerical model, a large number of experimental results reported by previous researchers were collected. The specimens were selected to display a wide range of material properties, such as the concrete strength, steel yield strength, and the ratio of the steel tube outer diameter to thickness, with the ratio of all specimen heights to sectional lengths being no more than 3, to eliminate the possible influence of buckling. The material properties and geometric details are presented in Table 1.

In Table 2, the results predicted by the proposed method N' and maximum experimental loads N_E are listed in detail, based on the 41 collected specimens. It can be observed that the predicted results are in strong agreement with the experimental results. The mean value of N'/N_E is 0.993, with a DEV of 0.049. Fig. 11 presents the comparison between the proposed theoretical predicted results N' and maximum experimental loads N_E.

The confining pressure provided by the steel tube f_r, expressed in Eq. (5), and the effective confining pressure provided by the peripheral stirrups f_{le}, expressed in Eq. (13), are indicated in Table 2. It can be observed that f_{le} and f_r generally have the same order of magnitude in the 41 ST-RC specimens. The percentage of f_{le}/f_r ranges from 12% to 70%, while the average percentage of f_{le}/f_r is equal to 32.10%, which confirms the assumption in Section 2 and indicates that the secondary confinement provided by peripheral hoop steel should be considered in the design of ST-RC columns. In actual projects, columns are required to have effective reinforcement so that seismic ductility and deformability can be ensured [44–46]. Therefore, it can be concluded that the confining pressure provided by the peripheral stirrups should be considered, particularly when the ST-RC column is effectively reinforced with transverse stirrups.

5. Comparison with existing methods

Four different methods based on the current leading design codes for calculating the axial capacity of ST-RC columns have been presented in this paper tentatively. The ST-RC column can be divided into two components, namely the outer RC and inner CFST components. The methods presented below are based on superimposing the respective bearing capacity of the core CFST and outer RC by means of existing formulae. It is worth noting that different standards use different methods to define the concrete compressive strength. The conversion relations among $f_{cyl,150}$ (ACI 318-14 and Eurocode 4-2004), $f_{cyl,100}$ (AIJ), and f_{ck} (CECS 188-2005) in the four standards follow the recommendation of Lu et al. [47]. Details of the calculation and comparison are elaborated as follows:

5.1. Method 1

Method 1 is suggested according to ACI 318-14 [48], in which the axial capacity of the RC encasement can be determined by Eq. (32). For the inner CFST component, ACI-318-14 [48] ignores the interaction between the concrete core and steel tube. The formula for evaluating the axial capacity of the CFST column is expressed as Eq. (33).

$$N_{RC,1} = 0.85 f_{cyl,\ 150,\ 1}(A_{RC} - A_{yl}) + f_{yl}A_{yl} \tag{32}$$

$$N_{CFST,1} = 0.85 f_{cyl,\ 150,\ 2}A_{core} + f_{ys}A_{ys} \tag{33}$$

where $f_{cyl,150,\ 1}$ and $f_{cyl,150,\ 2}$ denote the compressive strength of the outer concrete encasement and filled-in concrete without considering the confinement effect, respectively, obtained from 150 mm cylinder testes.

5.2. Method 2

Method 2 is investigated according to AIJ [49,50], where the ultimate compressive strengths of the axially loaded RC column and circular CFST column can be calculated by Eqs. (34) and (35), respectively. The axial capacity of the outer RC component is calculated as follows:

$$N_{RC,2} = 0.85 f_{cyl,\ 100,\ 1}(A_{RC} - A_{yl}) + f_{yl}A_{yl} \tag{34}$$

The axial capacity of the CFST component is calculated as follows:

$$N_{CFST,2} = 0.85 f_{cyl,\ 100,2}A_{core} + (1 + \eta) f_{ys}A_{ys} \tag{35}$$

where $f_{cyl,100,\ 1}$ and $f_{cyl,100,\ 2}$ denote the compressive strengths of the outer concrete encasement and filled-in concrete, without considering the confinement effect, respectively, obtained from 100 mm cylinder tests; η is the confinement factor taken as 0.27.

5.3. Method 3

Method 3 is suggested according to Eurocode 4-2004 [51]. For the outer RC component, the coefficient considering the long-term effects on compressive strength and of unfavorable effects resulting from the manner in which the load is applied ranges from 0.8 to 1.0 [52]. The strengths of the concrete and longitudinal bar are added simply in the RC columns. EC 4 [51] takes into account the confinement effect of the steel tube on the core concrete. The concrete strength is increased by the coefficient of confinement for concrete, η_c. The strength of the steel tube is decreased by the coefficient of confinement for the steel tube η_a owing to the hoop stress. According to EC 4 [51], the axial capacity of the circular CFST column can be calculated as:

$$N_{CFST,3} = \left(1 + \eta_c \frac{t}{D}\frac{f_{ys}}{f_{cyl,\ 150,\ 2}}\right) f_{cyl,\ 150,\ 2}A_{core} + \eta_a f_{ys}A_{ys} \tag{36}$$

Table 1
Summary of test data for ST-RC columns.

Number of specimens	B (mm)	D (mm)	t (mm)	f_{01} (MPa)	f_{02} (MPa)	f_{ys} (MPa)	f_{yv} (MPa)	s_l (mm)	n (mm)	s (mm)	Sources
8	200	127–133	1.5–4.5	51.8–53.9	51.8–53.9	270	391	160	2	100	Chen et al. [41]
18	220	89–114	2.6–5.1	36.3–51.8	75.2	316–360	391	180	2	40–60	Kang et al. [40]
4	150–170	60	2	39.1	39.1–51.7	325	380	110–130	2	100	Liu et al. [42]
6	250, 300	165, 219	2.6–3.6	27.6–30.0	28.6, 30.0	308–340	362	210, 260	2	50	Nie et al. [2]
5	400	200, 219	4.2–7.8	31.6–32.3	46.7	280–316	345, 376	120	4	100	Cai et al. [43]

Table 2
Test results and predicted axial capacity.

Source	Specimen label	f_{le} (MPa)	f_r (MPa)	f_{le}/f_r	N_E (kN)	Method 1		Method 2		Method 3		Method 4		Proposed method	
						N_1 (kN)	N_1/N_E	N_2 (kN)	N_2/N_E	N_3 (kN)	N_3/N_E	N_4 (kN)	N_4/N_E	N' (kN)	N'/N_E
Chen et al. [41]	A1-1	0.46	1.24	37%	2511	2003	0.798	2133	0.850	2189	0.872	2202	0.877	2469	0.984
	A1-2	0.46	1.24	37%	2447	2003	0.819	2133	0.872	2189	0.895	2202	0.900	2469	1.009
	B1-1	0.46	2.07	22%	2850	2164	0.759	2325	0.816	2446	0.858	2453	0.861	2647	0.929
	B1-2	0.46	2.07	22%	2992	2164	0.723	2325	0.777	2446	0.817	2453	0.820	2647	0.885
	C1-1	0.46	2.90	16%	2594	2221	0.856	2409	0.929	2593	1.000	2596	1.001	2702	1.042
	C1-2	0.46	2.90	16%	2761	2221	0.804	2409	0.873	2593	0.939	2596	0.940	2702	0.979
	D1-1	0.46	3.72	12%	2842	2287	0.805	2504	0.881	2745	0.966	2751	0.968	2767	0.974
	D1-2	0.46	3.72	12%	2906	2287	0.787	2504	0.862	2745	0.945	2751	0.947	2767	0.952
Kang et al. [40]	CC1	2.32	5.21	44%	3552	2711	0.763	2947	0.830	3197	0.900	3202	0.901	3619	1.019
	CC2	2.32	6.46	36%	4754	3513	0.739	3815	0.803	4028	0.847	4096	0.862	4539	0.955
	CC3	2.32	3.47	67%	3387	2595	0.766	2791	0.824	2972	0.878	2966	0.876	3490	1.030
	CC4	2.32	3.33	70%	4362	3115	0.714	3337	0.765	3458	0.793	3686	0.845	4101	0.940
	CC5	1.68	3.33	50%	3236	2585	0.799	2778	0.858	2953	0.913	2947	0.911	3325	1.027
	CC6	1.68	3.33	50%	3979	3115	0.783	3337	0.839	3458	0.869	3486	0.876	3946	0.992
	CC7	1.30	6.46	20%	3485	2787	0.800	3050	0.875	3336	0.957	3357	0.963	3425	0.983
	CC8	1.30	6.46	20%	4362	3513	0.805	3815	0.875	4028	0.923	3896	0.893	4271	0.979
	CC9	2.32	5.84	40%	3171	2403	0.758	2590	0.817	2690	0.848	2731	0.861	3267	1.030
	CC10	2.32	7.09	33%	3718	2433	0.654	2634	0.708	2742	0.738	3619	0.973	3671	0.987
	CC11	2.32	7.09	33%	3083	2433	0.789	2634	0.854	2742	0.889	2802	0.909	3294	1.068
	CC12	2.32	5.84	40%	3018	2403	0.796	2590	0.858	2690	0.891	2731	0.905	3267	1.083
	CC13	1.68	5.84	29%	3004	2403	0.800	2590	0.862	2690	0.895	2731	0.909	3109	1.035
	CC14	1.30	5.84	22%	2817	2405	0.854	2591	0.920	2691	0.955	2731	0.970	3007	1.068
	CC15	1.30	5.84	22%	3045	2403	0.789	2590	0.850	2690	0.883	2731	0.897	3006	0.987
	CC16	1.68	5.84	29%	3946	2989	0.758	3207	0.813	3247	0.823	3327	0.843	3797	0.962
	CC17	1.30	7.09	18%	2887	2362	0.818	2558	0.886	2674	0.926	2802	0.971	2946	1.020
	CC18	1.68	7.09	24%	3925	2362	0.602	2558	0.652	2674	0.681	3398	0.866	3528	0.899
Liu et al. [42]	R1-1	0.73	4.36	17%	1270	1011	0.796	1088	0.857	1102	0.868	1116	0.879	1212	0.954
	R1-2	0.73	4.36	17%	1252	1011	0.807	1088	0.869	1102	0.880	1116	0.891	1212	0.968
	R2-1	0.73	4.36	17%	1303	1037	0.796	1116	0.856	1133	0.870	1145	0.879	1241	0.952
	R2-2	0.73	4.36	17%	1274	1037	0.814	1116	0.876	1133	0.889	1145	0.899	1241	0.974
Nie et al. [2]	CDCFT1-1	1.25	2.31	54%	2763	2129	0.770	2335	0.845	2616	0.947	2581	0.934	2793	1.011
	CDCFT1-2	1.25	2.31	54%	2751	2201	0.800	2411	0.876	2691	0.978	2657	0.966	2877	1.045
	CDCFT1-3	1.25	2.31	54%	2732	2096	0.767	2300	0.842	2583	0.945	2547	0.932	2754	1.008
	CDCFT2-1	1.12	1.94	58%	3552	2941	0.828	3235	0.911	3698	1.041	3627	1.021	3882	1.093
	CDCFT2-2	1.12	1.94	58%	3614	3024	0.837	3323	0.919	3785	1.047	3715	1.028	3816	1.055
	CDCFT2-3	1.12	1.94	58%	3716	2930	0.789	3224	0.868	3687	0.992	3616	0.973	3870	1.042
Cai et al. [43]	FZ1	0.63	3.77	17%	7691	6484	0.843	7085	0.921	7742	1.007	7741	1.007	7743	1.007
	FZ2	0.63	3.89	16%	8052	6665	0.828	7290	0.905	7966	0.989	7951	0.988	7782	0.966
	FZ3	0.63	4.11	15%	8563	6980	0.815	7639	0.892	8347	0.975	8309	0.970	7847	0.916
	FZ4	0.63	2.35	27%	7490	5918	0.790	6355	0.849	6620	0.884	6641	0.887	6945	0.927
	FZ5	0.63	3.76	17%	8011	6590	0.823	7198	0.898	7824	0.977	7826	0.977	7688	0.960
Mean							0.786		0.852		0.907		0.921		0.993
DEV							0.048		0.054		0.075		0.053		0.049

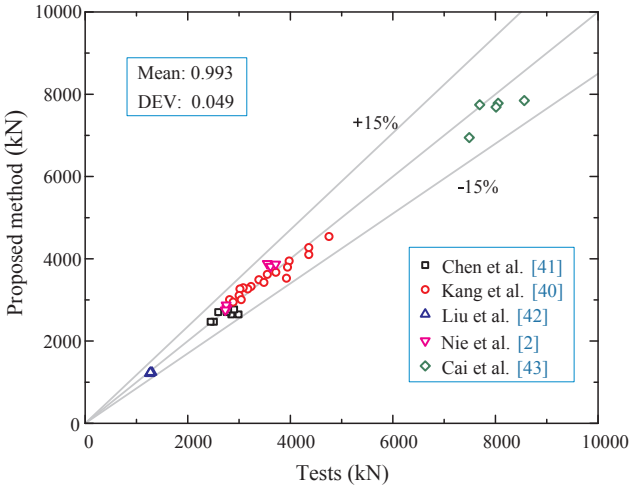

Fig. 11. Comparison of ultimate strengths between proposed method calculated results and test results.

in which

$$\eta_c = 4.9 - 18.5\bar{\lambda} + 17\bar{\lambda}^2 \tag{37}$$

$$\eta_a = 0.25(3 + 2\bar{\lambda}) \tag{38}$$

$$\bar{\lambda} = \sqrt{\frac{N_{plR}}{N_{cr}}} \tag{39}$$

$$N_{plR} = f_{ys}A_{ys} + f_{cyl,\ 150,\ 2}A_{core} \tag{40}$$

$$N_{cr} = \frac{\pi^2 (EI)_{eff2}}{l^2} \tag{41}$$

$$(EI)_{eff2} = E_s I_s + \kappa E_{c2} I_c \tag{42}$$

$$E_{c2} = 22,\ 000[(f_{cyl,\ 150,\ 2} + 8)/10]^{0.3} \tag{43}$$

where $\bar{\lambda}$ denotes the relative slenderness; l denotes the buckling length of the CFST column; E_{c2} denotes the elastic modulus of concrete in MPa; $(EI)_{eff2}$ denotes the effective flexural stiffness for the calculation of relative slenderness; and $\kappa = 0.6$ is a correction factor.

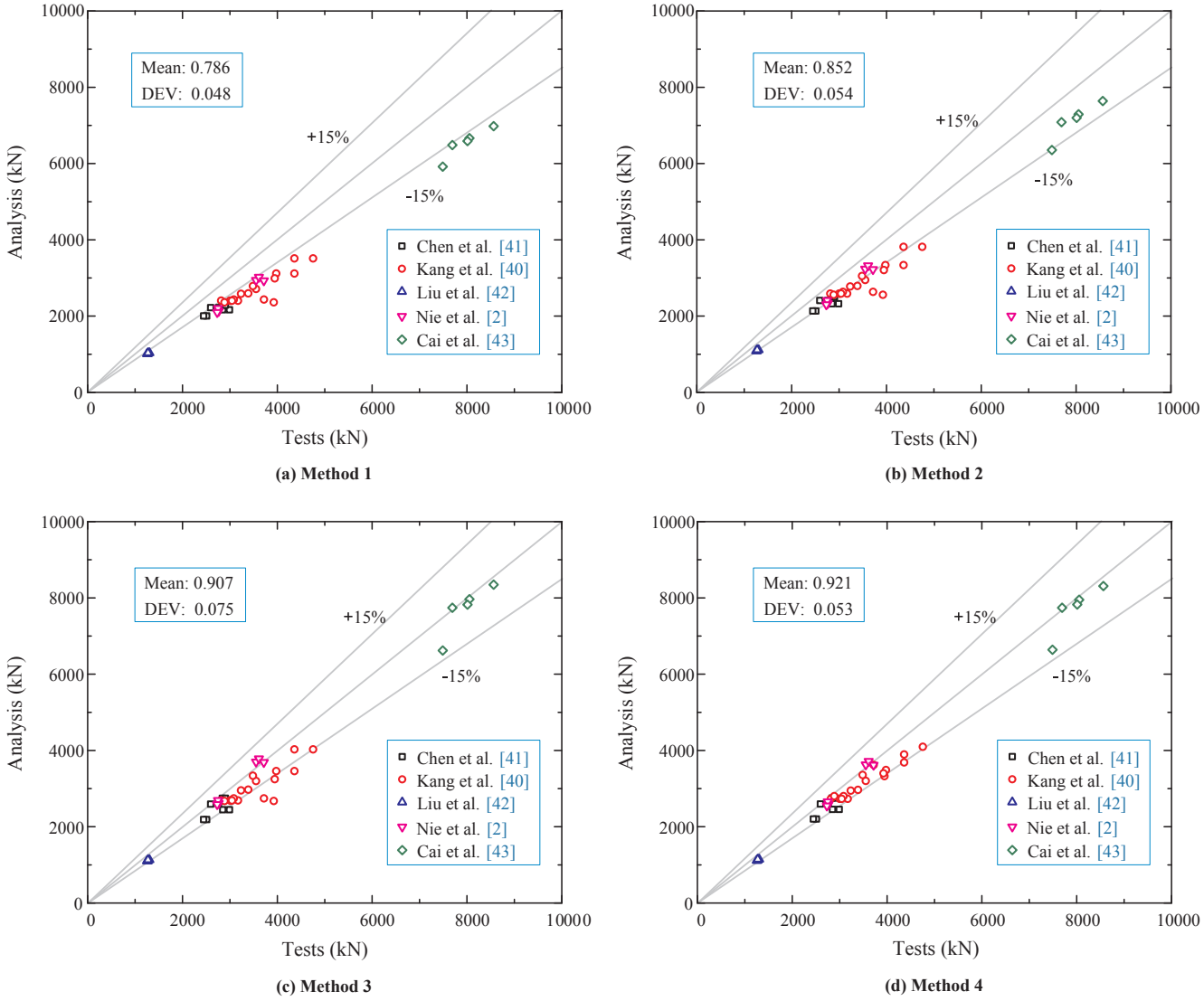

Fig. 12. Comparison of axial capacity between test results and predictions from four leading codes.

5.4. Method 4

Method 4 is implemented according to the Chinese code CECS 188-2005 [26], the technical specification developed for ST-RC concrete columns. The method is suggested as follows:

$$N_4 = 0.9 * \phi(f_{ck,\,1}A_{RC} + f_{yl}A_{yl}) + f_{ck,\,2}A_{core}(1 + 1.8\xi) \tag{44}$$

where $f_{ck,\,1}$ and $f_{ck,\,2}$ denote the characteristic concrete strength of the outer concrete encasement and filled-in concrete without considering the confinement effect, respectively; ϕ denotes the stability coefficient of the ST-RC column; and ξ denotes the confinement index of the steel tube, calculated as:

$$\xi = \frac{A_{ys}f_{ys}}{A_{core}f_{ck,\,2}} \tag{45}$$

Fig. 12 presents a comparison of the predictions of the four methods and maximum experimental loads. The four leading design codes exhibited slightly conservative predictions for the axial capacity of ST-RC columns. It was found that all of the design methods resulted in relatively conservative predictions. Method 1 (mean = 0.786, DEV = 0.048) exhibited the most conservative prediction of the ST-RC column axial capacity, because it ignored both the lateral confinement of concrete induced by the steel tube and transverse reinforcement. The predictions calculated by methods 2, 3, and 4 were close to one another, exhibiting errors of approximately 10% lower than the test results. The reason is that these three design methods only considered the lateral confinement induced by the steel tube, and ignored the lateral confinement of the transverse reinforcement. The empirical coefficients of confinements differed from one another, which led to discrepancies in the predicted results.

6. Conclusion

In this paper, the sectional equilibrium condition of the ST-RC column was elaborated based on the confining pressure interaction. It was found that, in general, the secondary confinement provided by the peripheral hoop steel has the same order of magnitude as the confining pressure provided by the steel tube: in 41 ST-RC specimens, the percentage of f_{le}/f_r ranged from 12% to 70%, and the average percentage of f_{le}/f_r was equal to 32.10%. This indicates that the secondary confinement effect of peripheral steel hoops should be considered in the design of ST-RC columns. Moreover, a modified method for predicting the axial capacity of the ST-RC column was developed by means of stress and strain analysis. By comparing the results predicted by the current method with a large number of specimens from different sources, it was found that the predicted results fitted strongly with the test results (the

mean value of N'/N_E was 0.993, with a DEV of 0.049). The four other methods according to ACI 318-14, AIJ, Eurocode 4-2004, and CECS 188-2005, were verified in the same scenario. Compared with conventional approaches, the proposed method correlated strongly with the experimental results. It is favorable to obtain the viable axial capacity of the ST-RC column by using the presented solution. However, as the current study only considered axially loaded ST-RC columns, there remains the need for studies taking into account combined axial compression and bending, which could form the future development of investigations into ST-RC columns.

Acknowledgments

This study was supported by National Natural Science Foundation of China (Grant No. 51478174) and the Fundamental Research Funds for the Central Universities (2016HNDX). These supports are gratefully acknowledged. Any opinions expressed in this paper are those of the writers and do not reflect the views of the sponsoring agencies.

Appendix A. Supplementary material

Supplementary data to this article can be found online at https://doi.org/10.1016/j.engstruct.2019.01.044.

References

[1] Ji X, Kang H, Chen X, Qian J. Seismic behavior and strength capacity of steel tube-reinforced concrete composite columns. Earthq Eng Struct Dyn 2014;43:487–505.
[2] Nie JG, Cai CS, Bai Y, Cai CS. New connection system for confined concrete columns and beams. I: experimental study. J Struct Eng 2008.
[3] Ji X, Zhang M, Kang H, Qian J, Hu H. Effect of cumulative seismic damage to steel tube-reinforced concrete composite columns. Earthq Struct 2014;7:179–99.
[4] Han LH, Li W, Bjorhovde R. Developments and advanced applications of concrete-filled steel tubular (CFST) structures: members. J Constr Steel Res 2014. https://doi.org/10.1016/j.jcsr.2014.04.016.
[5] Vu NS, Yu B, Li B. Stress-strain model for confined concrete with corroded transverse reinforcement. Eng Struct 2017. https://doi.org/10.1016/j.engstruct.2017.08.049.
[6] Samani AK, Attard MM. A stress-strain model for uniaxial and confined concrete under compression. Eng Struct 2012. https://doi.org/10.1016/j.engstruct.2012.03.027.
[7] Légeron F, Paultre P. Uniaxial confinement model for normal- and high-strength concrete columns. J Struct Eng 2003. https://doi.org/10.1061/(ASCE)0733-9445(2003) 129:2(241).
[8] Saatcioglu M, Razvi SR. Strength and ductility of confined concrete. J Struct Eng 1992. https://doi.org/10.1061/(ASCE)0733-9445(1992) 118:6(1590).
[9] Richart FE, Brandtzaeg A, Brown RL. Failure of plain and spirally reinforced concrete in compression. Bull. 190. Champaign: Univ. Illinois, Eng. Exp. Station; 1929.
[10] Mander JB, Priestley MJN, Park R. Theoretical stress-strain model for confined concrete. J Struct Eng 1988. https://doi.org/10.1061/(ASCE)0733-9445(1988) 114:8(1804).
[11] Razvi S, Saatcioglu M. Confinement model for high-strength concrete. J Struct Eng 1999. https://doi.org/10.1061/(ASCE)0733-9445(1999)125:3(281).
[12] Huang L, Yu T, Zhang S-S, Wang Z-Y. FRP-confined concrete-encased cross-shaped steel columns: concept and behaviour. Eng Struct 2017;152:348–58. https://doi.org/10.1016/j.engstruct.2017.09.011.
[13] Choi E, Jeon J-S, Cho B-S, Park K. External jacket of FRP wire for confining concrete and its advantages. Eng Struct 2013;56:555–66. https://doi.org/10.1016/j.engstruct.2013.05.019.
[14] Campione G, Fossetti M. Compressive behaviour of concrete elliptical columns confined by single hoops. Eng Struct 2007;29:408–17. https://doi.org/10.1016/j.engstruct.2006.05.006.
[15] Hassanein MF, Patel VI, El Hadidy AM, Al Abadi H, Elchalakani M. Structural behaviour and design of elliptical high-strength concrete-filled steel tubular short compression members. Eng Struct 2018;173:495–511. https://doi.org/10.1016/j.engstruct.2018.07.023.
[16] Leal G. JM, Pérez Gavilán JJ, Castorena G. JH, Velázquez D. JI. Infill walls with confining elements and horizontal reinforcement: an experimental study. Eng Struct 2017;150:153–65. https://doi.org/10.1016/j.engstruct.2017.07.042.
[17] Wu B, Zhang Q, Chen GM. Compressive behavior of thin-walled circular steel tubular columns filled with steel stirrup-reinforced compound concrete. Eng Struct 2018;170:178–95. https://doi.org/10.1016/j.engstruct.2018.05.028.
[18] Montuori R, Piluso V. Analysis and modelling of CFT members: moment curvature analysis. Thin-Walled Struct. 2015;86:157–66. https://doi.org/10.1016/j.tws.2014.10.010.
[19] Hu HS, Nie JG, Wang YH. Effective stiffness of rectangular concrete filled steel tubular members. J Constr Steel Res 2016. https://doi.org/10.1016/j.jcsr.2015.09.016.
[20] Kamil GM, Liang QQ, Hadi MNS. Local buckling of steel plates in concrete-filled steel tubular columns at elevated temperatures. Eng Struct 2018;168:108–18. https://doi.org/10.1016/j.engstruct.2018.04.073.
[21] Neuenschwander M, Knobloch M, Fontana M. Modeling thermo-mechanical behavior of concrete-filled steel tube columns with solid steel core subjected to fire. Eng Struct 2017;136:180–93.
[22] Romero ML, Espinos A, Portolés JM, Hospitaler A, Ibañez C. Slender double-tube ultra-high strength concrete-filled tubular columns under ambient temperature and fire. Eng Struct 2015;99:536–45.
[23] Han L, Wang Z, Xu W, Tao Z. Behavior of concrete-encased CFST members under axial tension. J Struct Eng 2016. https://doi.org/10.1061/(ASCE)ST.1943-541X.0001422.
[24] Han LH, An YF. Performance of concrete-encased CFST stub columns under axial compression. J Constr Steel Res 2014;93:62–76.
[25] Yuan H, Hong H-PH-P, Deng H, Bai Y. Displacement ductility of staged construction-steel tube-reinforced concrete columns. Constr Build Mater 2018;188:1137–48. https://doi.org/10.1016/j.conbuildmat.2014.07.086.
[26] CECS 188. Technical specification for steel tube-reinforced concrete column structure. China Planning Press; 2005.
[27] Karabinis AI, Rousakis TC. FRP confining effects on steel reinforced concrete square sections subjected to axial load. Fibre 2006.
[28] Montuori R, Piluso V. Reinforced concrete columns strengthened with angles and battens subjected to eccentric load. Eng Struct 2009;31:539–50. https://doi.org/10.1016/j.engstruct.2008.10.005.
[29] Montuori R, Piluso V, Tisi A. Comparative analysis and critical issues of the main constitutive laws for concrete elements confined with FRP. Compos Part B Eng 2012;43:3219–30. https://doi.org/10.1016/j.compositesb.2012.04.001.
[30] Montuori R, Piluso V, Tisi A. Ultimate behaviour of FRP wrapped sections under axial force and bending: influence of stress–strain confinement model. Compos Part B Eng 2013;54:85–96. https://doi.org/10.1016/j.compositesb.2013.04.059.
[31] He A, Cai J, Chen Q-J, Liu X, Xu J. Behaviour of steel-jacket retrofitted RC columns with preload effects. Thin-Walled Struct 2016;109:25–39. https://doi.org/10.1016/j.tws.2016.09.013.
[32] Chen S, Wu P. Analytical model for predicting axial compressive behavior of steel reinforced concrete column. J Constr Steel Res 2017.
[33] Liang QQ, Fragomeni S. Nonlinear analysis of circular concrete-filled steel tubular short columns under axial loading. J Constr Steel Res 2009. https://doi.org/10.1016/j.jcsr.2009.06.015.
[34] Sakino K, Nakahara H, Morino S, Nishiyama I. Behavior of centrally loaded concrete-filled steel-tube short columns. J Struct Eng 2004. https://doi.org/10.1061/(ASCE)0733-9445(2004) 130:2(180).
[35] Elremaily A, Azizinamini A. Behavior and strength of circular concrete-filled tube columns. J Constr Steel Res 2002;58:1567–91. https://doi.org/10.1016/S0143-974X(02)00005-6.
[36] Nakamura T, Wakabayashi M. A study on the superposition method to estimate the ultimate strength of steel reinforced concrete column subjected to axial thrust and bending moment simultaneously. Bull Disaster Prev Res Inst 1976;26.
[37] Wakabayashi M. Japanese standards for the design of composite buildings. Composite construction in steel & concrete. ASCE; 2010.
[38] Kwan AKH, Dong CX, Ho JCM. Axial and lateral stress–strain model for circular concrete-filled steel tubes with external steel confinement. Eng Struct 2016;117:528–41.
[39] Nematzadeh M, Fazli S, Naghipour M, Jalali J. Experimental study on modulus of elasticity of steel tube-confined concrete stub columns with active and passive confinement. Eng Struct 2017;130:142–53.
[40] Kang HZ. Study on mechanical properties of concrete-filled steel tube composite columns PhD Diss. Beijing: China Tsinghua Univ.; 2009.
[41] Chen ZY. Study of the method for design and calculation of HSC columns reinforced with concrete filled steel tube PhD Diss. Dalian: Dalian Univ. Technol.; 2002.
[42] Liu LY. Study on behavior of a new concrete-filled steel tube reinforced concrete column under axial compression Master Diss. Fuzhou: China Fuzhou Univ.; 2013.
[43] Cai J. An experimental research on the composite column with core of high-strength concrete filled steel tube under axial compression loading. J South China Univ Technol 2002;30:81–5.
[44] Hwang SK, Do Yun H. Effects of transverse reinforcement on flexural behaviour of high-strength concrete columns. Eng Struct 2004;26:1–12.
[45] Odijie AC, Quayle S, Ye J. Wave induced stress profile on a paired column semi-submersible hull formation for column reinforcement. Eng Struct 2017;143:77–90. https://doi.org/10.1016/j.engstruct.2017.04.013.
[46] Jing DH, Yu T, Liu XD. New configuration of transverse reinforcement for improved seismic resistance of rectangular RC columns: concept and axial compressive behavior. Eng Struct 2016;111:383–93.
[47] Lu ZH, Zhao YG. Suggested empirical models for the axial capacity of circular CFT stub columns. J Constr Steel Res 2010;66:850–62.
[48] ACI 318-14. Building code requirements for structural concrete and commentary. Am. Concr. Inst.; 2014.
[49] AIJ. Standards for structural calculation of steel reinforced concrete structures. 5th ed. Archit. Inst. Japan; 2001.
[50] AIJ. Recommendations for design and construction of concrete filled steel tubular structures. Archit. Inst. Japan; 1997.
[51] Eurocode 4. DESIGN of composite steel and concrete structures-Part1-1: general rules-structural rules for buildings. Brussels Eur. Comm. Stand.; 2004.
[52] Eurocode 2. Design of concrete structures-Part 1-1: general rules and rules for buildings. BS EN 1992-1-12004 Eur. Comm. Stand.; 2004.